Journal of Electrochemistry

Volume 27 | Issue 6

2021-12-28

Photoelectrochemical Sensing Based on Zr-MOFs for Homocysteine Detection

Wen-Xia Dong

Guang-Ming Wen

1. School of Chemistry and Chemical Engineering, Jinzhong University, Jinzhong, 030600, Shanxi, China;2. Institute of Environmental Science and School of Chemistry and Chemical Engineering, Shanxi University, Taiyuan 030006, Shanxi, China; wgm@sxu.edu.cn

Bin Liu

Zhong-Ping Li

DOI: Due to the independent format of the light source and detection system, photoelectrochemical (PEC) sensor has the advantages of low background, high sensitivity and simple operation. So far, PEC systems have been widely used in the fields including the actual detection of metal ions, biological antibodies or antigens in environmental pollutants. When the photosensitive material is irradiated by a light source with an energy being equal to or greater than its band gap, electrons (e^-) transition occurs from the valence band to the conduction band, leaving a hole (h^+), at the same time, the generated electron-hole pair (e^-/h^+) separate, and migrate to the electrode surface and electrolyte to generate photocurrent or photovoltage. When the target analyte is added, it will interact with its recognition molecule, and affect the separation or migration process of the charge, thereby, causing a change in the photocurrent. Metal organic framework (MOF) is a material composed of metal ions and organic linking groups. They have adjustable porosity, functional surface and massive conjugate back bone. These unique characteristics of MOF have been extensively explored in various fields. Zr-MOFs were synthesized use 4-carboxyphenylporphyrin (TCPP) as the ligand, and metal zirconium (Zr) as the coordination metal. Using Zr-MOFs as the photoelectrically active material, a cathode photoelectrochemical sensor was constructed to detect homocysteine (Hcy). A three-electrode system, consisting of Zr-MOFs/FTO electrode, Pt electrode and Ag/AgCl electrode, was inserted into 0.01 $mol \cdot L^{-1}$ HEPES solution to prepare the sensor. An aqueous solution of homocysteine was added to the electrolyte, allowing it to stand for 5 min. Cyclic voltammetry and electrochemical impedance spectroscopy were used to characterize the reaction process and the electron transfer process between optoelectronic materials. When the Xe lamp with λ > 420 nm is used to irradiate Zr-MOFs, electrons (e^-) in the valence band transfer to the conduction band, and holes (h^+) are generated in the valence band, thereby, generating light current. The addition of homocysteine will hinder the transfer of electrons, causing the cathode photocurrent to be decreased. The prepared sensor had good linear responses in the ranges of 10 ~ 100 $nmol \cdot L^{-1}$ and 100 ~ 1000 $nmol \cdot L^{-1}$, and the detection limit was 2.17 $nmol \cdot L^{-1}$. The sensor also exhibited good stability and selectivity. The prepared cathode photoelectric sensor could sensitively and efficiently detect homocysteine in milk. The studied high-performance photoelectric active materials and chemical sensing platforms may be important for the design of other chemical sensing platforms and the development of PEC applications.

第 27 卷 第 6 期
2021 年 12 月

电化学
JOURNAL OF ELECTROCHEMISTRY

Vol. 27 No. 6
Dec. 2021

【Article】 **DOI**: 10.13208/j.electrochem.210126 **Http**://electrochem.xmu.edu.cn

基于 Zr-MOFs 光电化学传感用于同型半胱氨酸的检测

董文霞[1,2],温广明[1,2*],刘 斌[2],李忠平[2]
(1. 晋中学院化学化工学院,山西 榆次 030600;2. 山西大学化学化工学院,山西 太原 030006)

摘要: 以 4-羧基苯基卟啉(TCPP)作为配体,金属锆(Zr)作为配位金属,通过水热法合成 Zr-MOFs。以 Zr-MOFs 材料作为光电活性材料构建了阴极光电化学传感器用于检测同型半胱氨酸(Hcy)。当 $\lambda > 420$ nm 的氙灯光源照射 Zr-MOFs 时,处于价带(VB)上的电子(e^-)跃迁至导带(CB),并在价带上产生空穴(h^+),从而产生光电流。同型半胱氨酸的加入会阻碍电子的传递,从而造成阴极光电流降低。当目标物浓度为 10 ~ 100 nmol·L^{-1} 和 100 ~ 1000 nmol·L^{-1} 时,光电流信号变化值与目标物浓度呈线性关系,且检出限为 2.17 nmol·L^{-1},制备的传感器具有良好的稳定性和选择性。

关键词: 阴极光电流;Zr-MOFs;同型半胱氨酸

1 引 言

光电化学(PEC)分析方法将光化学与电化学方法相结合,以光源作为激发源,激发光电活性材料产生电子-空穴对,从而产生光电流信号。因此,光电化学具有低背景和高灵敏度等优点[1-4]。当光电材料被光激发产生电子-空穴对的同时,其中一部分电荷将重新组合而形成较低的光电流[5-7]。然而,电子供体的存在会清理部分空穴,从而改善光电流强度。多巴胺(DA)已经被发现是一种优异的电子供体[8-10]。光电活性材料的选择对于 PEC 传感器具有重要的作用。金属有机骨架(MOFs)因其独特的多孔性及光电性质近年来被广泛应用于光电化学传感方面[11-16]。

同型半胱氨酸(Hcy)是一种含硫氨基酸,是血管损害的敏感指标,也是糖尿病早期诊断的重要指标。体内 Hcy 的量已经被认为是心血管疾病的最强有力的警报[17-22]。近几年,已经开发出多种检测含硫醇氨基酸的实验方法,包括紫外可见吸光光度法[23]、荧光法[24]和磷光法[25]。

本文以 $ZrCl_4$ 为原料,4-羧基苯基卟啉(TCPP)为配体通过化学法合成 Zr-MOFs,合成的 Zr-MOFs 具有优异的光电活性。基于 Zr-MOFs 和 Hcy 之间的反应导致阴极光电流降低,该体系具有良好的选择性和较高的灵敏度。

2 实 验

2.1 试剂与仪器

紫外可见吸收光谱使用 U-2910 分光光度计(日立,日本东京)记录。使用 JSM-7900F(日本电子,日本)生成扫描电子显微镜(TEM)图像。X 射线衍射图(XRD)由具有石墨单色 Cu K_α 辐射(λ = 0.154 nm)的 Rigaku Dmax 2000 X 射线衍射仪(理学电企仪器有限公司,北京)获得。PEC 检测在

引用格式: Dong W X, Wen G M, Liu B, Li Z P. Photoelectrochemical sensing based on Zr-MOFs for homocysteine detection. *J. Electrochem.*, 2021, 27(6): 681-688.

收稿日期: 2021-01-26,修订日期: 2021-05-13. * 通讯作者, Tel: (86-351)3985596, E-mail: wgm@sxu.edu.cn
2019 年山西省优秀研究生创新项目(No. 2019SY018)、晋中学院创新团队项目(No. jzxycxtd2019007)、南京大学“生命分析化学国家重点实验室”2019 年度开放研究项目(No. SKLACLS1911)和第“十二批”山西省百人计划项目(128,129)项目资助

RST5200F 电化学工作站(郑州世瑞思仪器科技有限公司,郑州)上进行。氙灯(北京中教金源科技有限公司,北京)(λ > 420 nm)作为光源。

FTO 玻璃(15 × 50 mm,电阻为 10 Ω)(武汉晶格太阳能科技有限公司,中国);氯化锆(98%)、苯甲酸(≥ 99.9%)、卟啉(TCPP)(98%)、N,N-二甲基甲酰胺(DMF,分析纯)、多巴胺(DA,98%)、4-羟乙基哌嗪乙磺酸(HEPES,> 99%)均购自上海阿拉丁生化科技股份有限公司;实验所用二次水均来自 Millipore 净水系统(≥ 18 MΩ·cm,Milli-Q,Millipore)。

2.2 光电材料的制备

将 $ZrCl_4$(75 mg)、TCPP(30 mg)和苯甲酸(1750 mg)溶解在 10 mL DMF 中,并将上述溶液超声溶解在玻璃小瓶中。将上述混合物加热至 120 ℃,保持 48 h。将合成的材料冷却至室温,在离心条件下收集紫色针状晶体[26]。将 0.005 g Zr-MOFs 超声溶解于 5 mL 甲醇中分散 2 h,并在 4 ℃ 下保存。

2.3 传感器的制备

将 FTO 电极在丙酮,乙醇和二次水中分别超声清洗 30 min,然后将清洗后的 FTO 电极存放于乙醇溶液中,备用。将 1 g·L^{-1} Zr-MOFs 溶液滴涂于 FTO 电极上。Zr-MOFs/FTO 电极、Pt 电极和 Ag/AgCl 电极构成三电极系统,并将该三电极系统插入 0.01 mol·L^{-1} HEPES 溶液中制备传感器。打开/关闭 Xe 灯光源测试 60 s,重复上述实验多次,直到光电流稳定为止。将同型半胱氨酸的水溶液添加到电解质中,静置 5 min 进行检测。

3 结果与讨论

3.1 传感过程

使用 Zr-MOFs 作为光电活性材料构建阴极光电化学传感器,同型半胱氨酸(Hcy)的加入形成“信号关闭”的光电流响应,在所制备的传感器中,阴极光电流随着 Hcy 的加入逐渐降低。为了进一步获得 Zr-MOFs/FTO 电极上 Hcy 反应的信息,通过设置扫描速率为 0.6 V·s^{-1}、电流量程为 10^{-2} A 的循环伏安曲线研究了扫描速率的影响。研究同型半胱氨酸(Hcy)的氧化峰值电流对扫描速率的依赖性,来评估反应机理。设置扫描速率从 30 到 600 mV·s^{-1},通过 CV 技术研究了在含有 Hcy(100 nmol·L^{-1})的 0.01 mol·L^{-1} HEPES 溶液中的电化学行为。所得的伏安图如图 1(A)所示,Hcy 的氧化峰值电势随扫描速率的增加而正移。从图 1(B)看出,氧化峰电流 I 与扫描速率 v 之间存在良好的线性关系,线性回归方程为 $y = 0.483 \times 10^{-3}x + 0.145$,$R^2 = 0.991$,显示该过程是典型的吸附过程,这说明 Hcy 吸附到电极表面后会阻碍电子间的传递,从而形成阴极光电流降低的现象。

3.2 光电材料的表征

我们采用透射电子显微镜(TEM)和扫描电子显微镜(SEM)表征了 Zr-MOFs 的形态,从图 2(A)和图 2(B)中我们可以发现 Zr-MOFs 约为 3 ~ 4 μm 的棒状结构。X 射线衍射图(图 3(A))观察到 Zr-MOFs 的主要衍射峰 2.4°、4.8°、7.1° 和 9.8°[27]均存在。从图 3(B)中可以看出,在 200 ~ 800 nm 范围内 Zr-MOFs 具有较强的吸收,这表明 Zr-MOFs 可

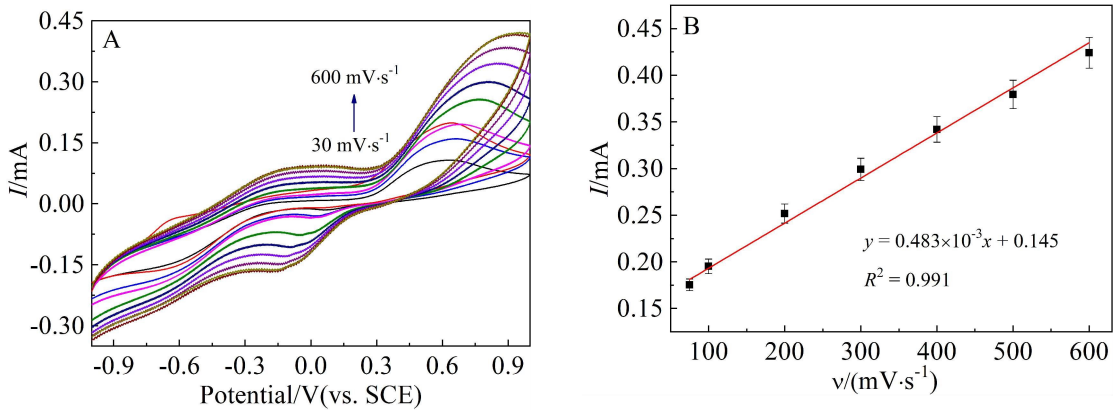

图 1 (A)Zr-MOFs/FTO 电极上不同扫描速率(30、50、75、100、200、300、400、500 和 600 mV·s^{-1})在 0.01 mol·L^{-1} HEPES 中的循环伏安图。(B)峰电流值与扫描速率的线性拟合曲线。(网络版彩图)

Figure 1 (A) Cyclic voltammograms at different scan rates (30, 50, 75, 100, 200, 300, 400, 500 and 600 mV·s^{-1}) on Zr-MOFs/FTO electrodes in 0.01 mol·L^{-1} HEPES. (B) Linear fitting plot of peak current and scan rate. (color on line)

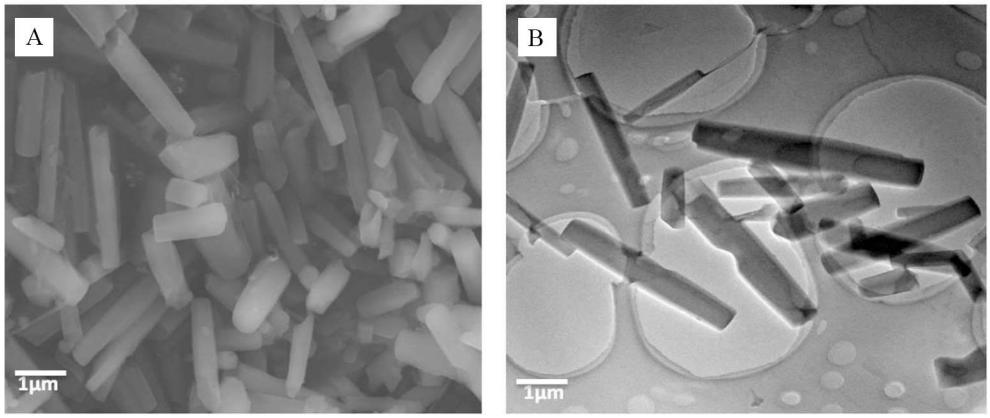

图 2（A)Zr-MOFs 的扫描电镜图;(B)Zr-MOFs 的透射电镜图

Figure 2 (A) SEM image of Zr-MOFs; (B) TEM image of Zr-MOFs

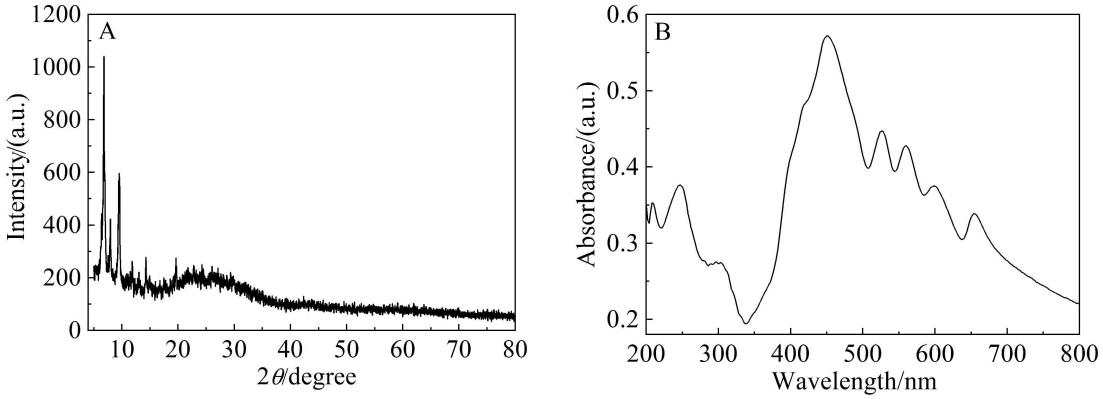

图 3 (A) Zr-MOFs 的 XRD 图;(B)Zr-MOFs 的紫外可见吸收光谱图

Figure 3 (A) XRD pattern of Zr-MOFs; (B) UV-Vis absorption spectrum of Zr-MOFs

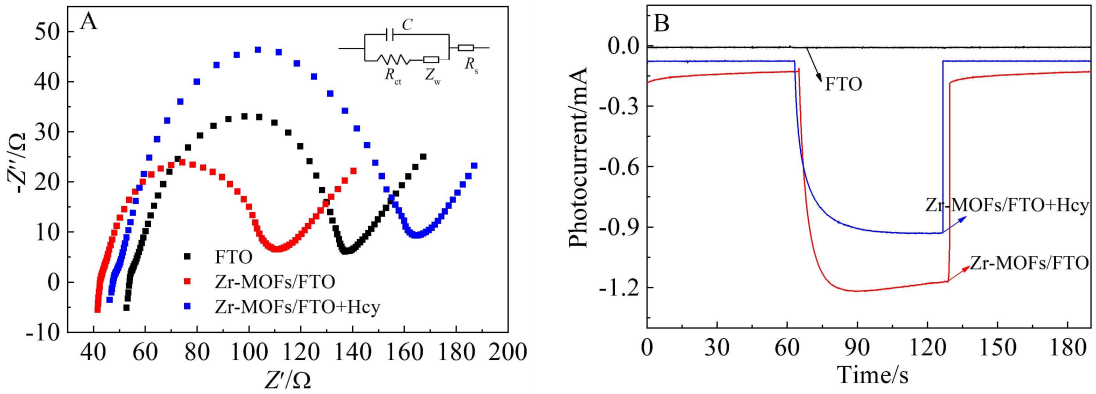

图 4（A)FTO、Zr-MOFs/FTO 和 Zr-MOFs/FTO+Hcy 的阻抗图;(B)FTO,Zr-MOFs/FTO 和 Zr-MOFs/FTO+Hcy 的光电流响应图。（网络版彩图）

Figure 4 (A) Nyquist plots of FTO, Zr-MOFs/FTO and Zr-MOFs/FTO+Hcy (the inset is an equivalent circuit); (B) Photocurrent responses of FTO, Zr-MOFs/FTO and Zr-MOFs/FTO+Hcy. (color on line)

以在可见光下进行有效的电子跃迁[28, 29]。

电化学阻抗谱图(EIS)是表征电极材料电阻性质的一种有效方法，实验过程中设置偏置电位为 0.2375 V,起始频率为 100000 Hz,交流振幅为 0.007 V。图 4(A)显示了在含有 0.1 mol·L^{-1} KCl 的 5 mmol·L^{-1} $Fe(CN)_6^{3-/4-}$ 溶液中构建的 EIS 图。插图是等效电路图，该电路由电极和电解质的双层电容器(C)、溶液电阻(R_s)、电子转移电阻(R_{et})和 Warburg 阻抗(Z_w)组成。如图 4(A)所示,裸 FTO 电极的阻值约为 80 Ω,将 Zr-MOFs 滴涂于 FTO 电极时,Zr-MOFs/FTO 的阻值约为 70 Ω，这说明 Zr-MOFs 具有良好的导电性。将制备好的电极浸入到含有 100 nmol·L^{-1} Hcy 溶液 20 min 后,我们发现 Zr-MOFs/FTO+Hcy 的阻值增大到 120 Ω，说明加入 Hcy 后电子转移阻力进一步地增大，导致其阻抗值增加。Zr-MOFs/FTO 和 Zr-MOFs/FTO+Hcy 的光电流值如图 4(B)所示,从图中我们不难发现 Zr-MOFs/FTO 比 Zr-MOFs/FTO+Hcy 具有更强的阴极光电流,这与阻抗图的结果一致。

3.3 传感器的条件优化以及性能表征

为了研究该传感器的性能，对 Zr-MOFs 的修饰量进行了优化。如图 5(A)所示,当 Zr-MOFs 的修饰量为 50 μL 时,光电流显示出最高值,因此后续实验中 Zr-MOFs 的修饰量均为 50 μL。为了评估传感器的稳定性和重现性，将制备好的传感器在开光/避光下重复测试 15 次，发现该传感器在 30 min 内有良好的稳定性(图 5(B))。通过测试传感器在 0.01 mol·L^{-1} HEPES 条件下的光电流响应，如图 5(C)所示,说明该传感器具有良好的重现性。

3.4 光电化学传感器对 Hcy 的检测

向上述制备好的三电极系统中依次加入 Hcy，不同浓度的光电流响应如图 6(A)所示,不难发现随着 Hcy 的增加阴极光电流在逐渐降低。图 6(B)为光电响应值与 Hcy 浓度的线性关系曲线，二者在 10 ~ 100 nmol·L^{-1} 和 100 ~ 1000 nmol·L^{-1} 范围内呈良好的线性关系,线性方程分别为 y = 7.896×

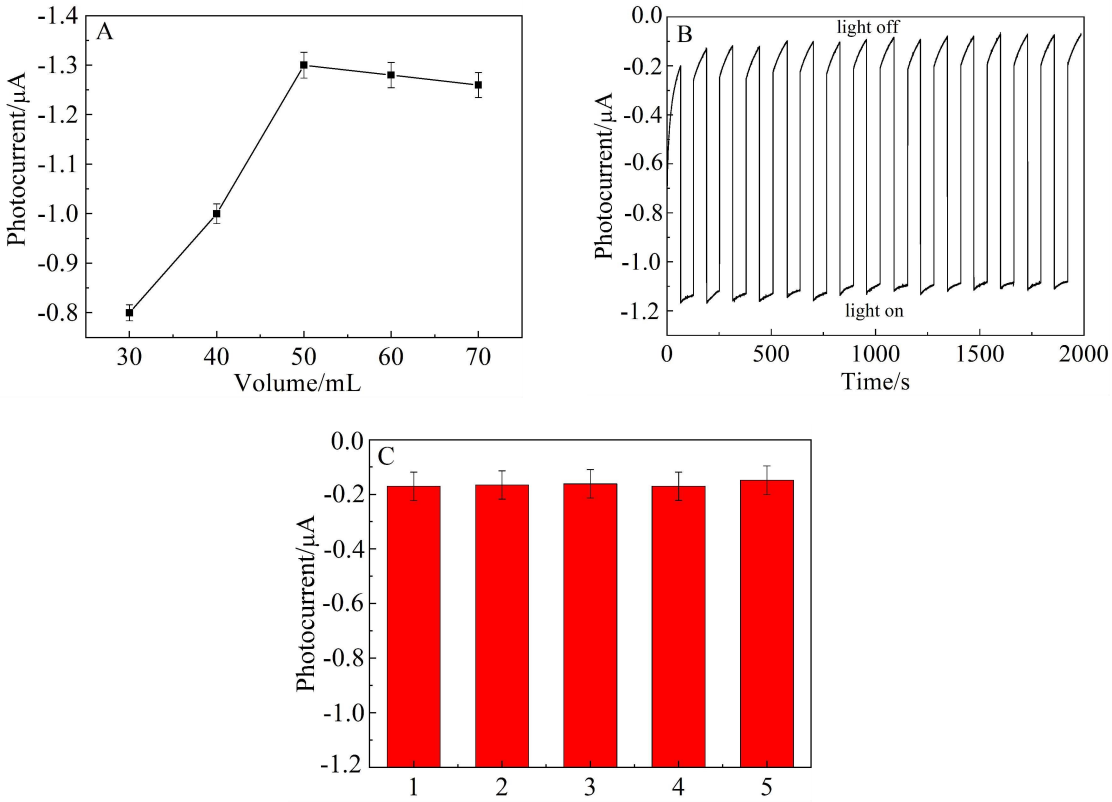

图 5　(A)Zr-MOFs 修饰量的优化(1 g·L^{-1} Zr-MOFs 的修饰量依次为 30 μL、40 μL、50 μL、60 μL、70 μL);(B)传感器的稳定性(设置电压为 0 V);(C)传感器的重现性 (网络版彩图)

Figure 5　(A) Optimization of Zr-MOFs modification amount (the modification amount of 1 g·L^{-1} Zr-MOF: 30 μL, 40 μL, 50 μL, 60 μL, 70 μL); (B) Sensor stability data (setting voltage to 0 V); (C) Sensor reproducibility data (color on line)

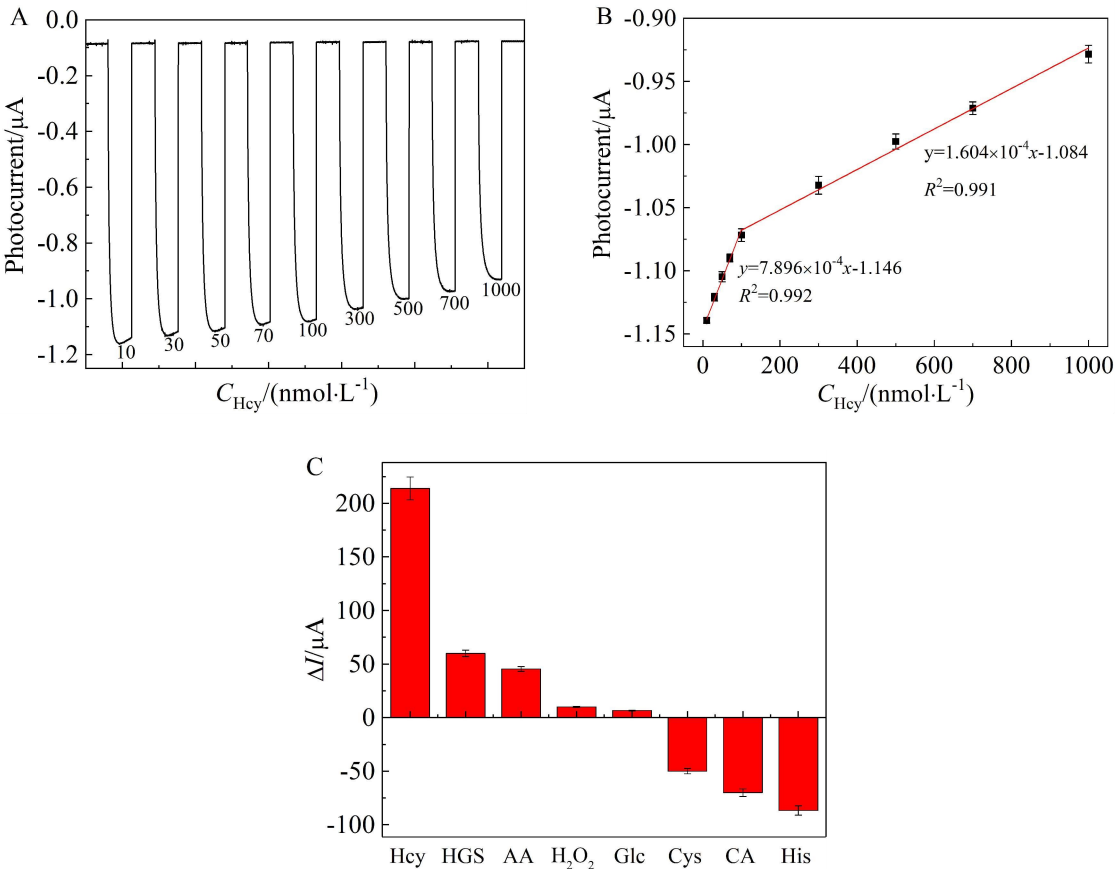

图 6（A)传感器对不同浓度 Hcy 的光电流响应曲线;(B)光电流与 Hcy 浓度的线性关系曲线;(C) 传感器测定 Hcy 的抗干扰性。(网络版彩图)

Figure 6 (A) Photocurrent response curve of the sensor to different concentrations of Hcy; (B) Linear relationship of photocurrent and Hcy concentration; (C) The anti-interference of Hcy measured by the sensor. (color on line)

表 1 不同的方法及材料用于检测 Hcy

Table 1 Methods and materials used to detect Hcy

Material	Method	Linear range	Detection limit	Ref.
CdTe/CdS	Fluorescence on-off	1 ~ 90 μmol·L^{-1}	0.67 μmol·L^{-1}	30
Au NPs	Electrochemical	0.05 ~ 20.0 μmol·L^{-1}	0.01 μmol·L^{-1}	31
BIHM	Fluorescence probe	-	9.02×10^{-6} mol·L^{-1}	32
Zr-MOFs	Photoelectrochemical	10 ~ 1000 nmol·L^{-1}	2.17 nmol·L^{-1}	This work

10^{-4}-1.146,R^2 = 0.992 和 y = 1.604×10^{-4}-1.084,R^2 = 0.991,检出限为 2.17 nmol·L^{-1}。与现有的检测 Hcy 的荧光开关法[31]、电化学方法[32]、荧光探针法[33]相比，设计的光电化学传感器用于检测 Hcy 时具有更低的检出限和更宽的线性范围。图 6(C)显示了存在 300 nmol·L^{-1} 其他干扰物质(谷胱甘肽,抗坏血酸,H_2O_2,葡萄糖,半胱氨酸,柠檬酸和组氨酸)对检测 100 nmol·L^{-1} 同型半胱氨酸时的影响。实验发现，加入 100 nmol·L^{-1} Hcy 时阴极光电流降低约 214 μA。加入 300 nmol·L^{-1} 谷胱甘肽、抗坏血酸、H_2O_2 和葡萄糖时阴极光电流分别降低约 60 μA、45.5 μA、10 μA、6.67 μA、,加入 300 nmol·L^{-1} 半胱氨酸,柠檬酸和组氨酸时,阴极光电流分别升高 50 μA、70 μA、86.67 μA。结果表明,这些干扰物的存

表 2 牛奶中同型半胱氨酸的检测

Table 2 Detection of homocysteine in milk

Sample	Added/(nmol·L^{-1})	Found/(nmol·L^{-1})	Recovery/%	RSD/%
Milk	30	28.78	104.24	3.41
	100	101.23	98.78	2.80
	300	298.98	100.34	1.76

在对同型半胱氨酸的检测影响较小。设计的光电化学传感器可以对 Hcy 进行高灵敏、高选择的检测。

3.5 牛奶中 Hcy 的检测

为了研究制备的 PEC 传感器在牛奶样品中的实际应用，将一定量的牛奶稀释到 0.01 mol·L^{-1} HEPES 溶液中，并添加不同浓度(30、100 和 300 nmol·L^{-1})的 Hcy 进行加标回收实验。如表 1 所示，回收率达到 98.78 ~ 104.24%，相对标准偏差(RSD，n = 3)为 1.76 ~ 3.41%。结果表明，我们提出的传感平台对牛奶样品中 Hcy 的检测具有可行性且其他样品对牛奶中 Hcy 的检测没有影响。

4 结　论

首次构建了通过一步水热法合成 Zr-MOFs 作为光电活性材料用于检测 Hcy 的阴极光电流传感器。Zr-MOFs 较窄的带隙可有效阻止光电子的复合，从而形成较强的光电流，Hcy 的加入通过在电极表面的吸附，从而有效抑制了阴极光电流的产生。设计的阴极传感器的光电流与 Hcy 的浓度在 10 ~ 100 nmol·L^{-1} 和 100 ~ 1000 nmol·L^{-1} 内呈现良好的线性关系。

参考文献(References):

[1] Shu J, Qiu Z L, Zhou Q, Lin Y X, Lu M H, Tang D P. Enzymatic oxydate-triggered self-illuminated photoelectrochemical sensing platform for portable immunoassay using digital multimeter[J]. Anal. Chem., 2016, 88(5): 2958-2966.

[2] Li Y, Zhang N, Zhao W W, Jiang D C, Xu J J, Chen H Y. Polymer dots for photoelectrochemical bioanalysis[J]. Anal. Chem., 2017, 89(9): 4945-4950.

[3] Zhao C Q, Ding S N, Xu J J, Chen H Y. ZnAgInS quantum dot-decorated BiOI heterostructure for cathodic photoelectrochemical bioanalysis of glucose oxidase[J]. ACS Appl. Nano Mater., 2020, 3(11): 11489-11496.

[4] Yan K, Liu Y, Yang Y H, Zhang J D. A cathodic "signal-off" photoelectrochemical aptasensor for ultrasensitive and selective detection of oxytetracycline[J]. Anal. Chem., 2015, 87(24): 12215-12220.

[5] Wu S, Song H L, Song J, He C, Ni J, Zhao Y Q, Wang X Y. Development of triphenylamine functional dye for selective photoelectrochemical sensing of cysteine[J]. Anal. Chem., 2014, 86(12): 5922-5928.

[6] Li Z P, Dong W X, Du X Y, Wen G M, Fan X J. A novel photoelectrochemical sensor based on g-C_3N_4@CdS QDs for sensitive detection of Hg^{2+}[J]. Microchem. J., 2020, 152: 104259.

[7] Yu S Y, Zhang L, Zhu L B, Gao Y, Fan G C, Han D M, Chen G X, Zhao W W. Bismuth-containing semiconductors for photoelectrochemical sensing and biosensing[J]. Coord. Chem. Rev., 2019, 393: 9-20.

[8] Gao C M, Xue J, Zhang L, Cui K, Li H, Yu J H. Paper-based origami photoelectrochemical sensing platform with TiO_2/Bi_4NbO_8Cl/Co-Pi cascade structure enabling of bidirectional modulation of charge carrier separation[J]. Anal. Chem., 2018, 90(24): 14116-14120.

[9] Hao Q, Wang P, Ma X Y, Su M Q, Lei J P, Ju H X. Charge recombination suppression-based photoelectrochemical strategy for detection of dopamine[J]. Electrochem. Commun., 2012, 21: 39-41.

[10] Cooper D R, Suffern D, Carlini L, Clarke S J, Parbhoo R, Bradforth S E, Nadeau J L. Photoenhancement of lifetimes in CdSe/ZnS and CdTe quantum dot-dopamine conjugates [J]. Phys. Chem. Chem. Phys., 2009, 11(21): 4298-4310.

[11] Deria P, Gómez-Gualdrón D A, Hod I, Snurr R MQ, Hupp J T, Farha O K. Framework-topology-dependent catalytic activity of zirconium-based (porphinato)zinc(II) MOFs[J]. J. Am. Chem. Soc., 2016, 138(43): 14449-14457.

[12] Chen J, Chen H Y, Wang T S, Li J F, Wang J, Lu X Q. Copper ion fluorescent probe based on Zr-MOFs composite material[J]. Anal. Chem., 2019, 91(7): 4331-4336.

[13] Wang J H, Li M N, Yan S, Zhang Y, Liang C C, Zhang X M, Zhang Y B. Modulator-induced Zr-MOFs diversification and investigation of their properties in gas sorption and Fe^{3+} ion sensing[J]. Inorg. Chem., 2020, 59(5): 2961-2968.

[14] Gao Y, Wu J F, Wang J Q, Fan Y X, Zhang S Y, Dai W. A novel multifunctional p-type semiconductor@MOFs nanoporous platform for simultaneous sensing and photodegradation of tetracycline[J]. ACS Appl. Mater. Interfaces, 2020, 12(9): 11036-11044.

[15] Xu G L, Zhang H B, Wei J, Zhang H X, Wu X, Li Y, Li C S, Zhang J, Ye J H. Integrating the g-C_3N_4 nanosheet with B-H bonding decorated metal-organic framework for CO_2 activation and photoreduction[J]. ACS Nano, 2018, 12(6): 5333-5340.

[16] Zhang G Y, Zhuang Y H, Shan D, Su G F, Cosnier S, Zhang X J. Zirconium-based porphyrinic metal-organic framework (PCN-222): enhanced photoelectrochemical response and its application for label-free phosphoprotein detection[J]. Anal. Chem., 2016, 88(22): 11207-11212.

[17] Zhu Y H, Xu Z W, Yan K, Zhao H B, Zhang J D. One-step synthesis of CuO-Cu_2O heterojunction by flame spray pyrolysis for cathodic photoelectrochemical sensing of L-cysteine[J]. ACS Appl. Mater. Interfaces, 2017, 9(46): 40452-40460.

[18] Michael J, MacCoss N K. Measurement of homocysteine concentrations and stable isotope tracer enrichments in human plasma[J]. Anal. Chem., 1999, 71(20): 4527-4533.

[19] Wang Y Q, Wang W, Wang S S, Chu W J, Wei T, Tao H J, Zhang C X, Sun Y M. Enhanced photoelectrochemical detection of L-cysteine based on the ultrathin polythiophene layer sensitized anatase TiO_2 on F-doped tin oxide substrates[J]. Sensor. Actuat. B - Chem., 2016, 232: 448-453.

[20] Hubmacher D, Sabatier L, Annis D S, Mosher D F, Reinhardt D P. Homocysteine modifies structural and functional properties of fibronectin and interferes with the fibronectin-fibrillin-1 interaction[J]. Biochem., 2011, 50 (23): 5322-5332.

[21] Ozoemena K, Westbroek P, Nyokong T. Long-term stability of a gold electrode modified with a self-assembled monolayer of octabutylthiophthalocyaninato-cobalt (II) towards L-cysteine detection[J]. Electrochem. Commun., 2001, 3(9): 529-534.

[22] Magdalena S, Anthony A M, Agata C, Maria H. Mercury/homocysteine ligation-induced ON/OFF-switching of a T-T mismatch-based oligonucleotide molecular beacon[J]. Anal. Chem., 2012, 84(11): 4970-4978.

[23] Gates A T, Fakayode S O, Lowry M, Ganea G M, Murugeshu A, Robinson J W, Strongin R M, Warner I M. Gold nanoparticle sensor for homocysteine thiolactone-induced protein modification[J]. Langmuir, 2008, 24(8): 4107-4113.

[24] Zhang M, Yu M X, Li F Y, Zhu M W, Li M Y, Gao Y H, Li L, Liu Z Q, Zhang J P, Zhang D Q, Yi T, Huang C H. A highly selective fluorescence turn-on sensor for cysteine/homocysteine and its application in bioimaging[J]. J. Am. Chem. Soc., 2007, 129(34): 10322-10323.

[25] Chen H L, Zhao Q, Wu Y B, Li F Y, Yang H, Yi T, Huang C H. Selective phosphorescence chemosensor for homocysteine based on an iridium(III) complex[J]. Inorg. Chem., 2007, 46(26): 11075-11081.

[26] Feng D W, Gu Z Y, Li J R, Jiang H L, Wei Z W, Zhou H C. Zirconium-metalloporphyrin PCN-222: Mesoporous metal-organic frameworks with ultrahigh stability as biomimetic catalysts[J]. Angew. Chem. Int. Ed., 2012, 51 (41): 10307-10310.

[27] Bonnett B L, Smith E D, Cai M, Haag J V, Serrano J M, Cornell H D, Gibbons B, Martin S M, Morris A J. PCN-222 metal-organic framework nanoparticles with tunable pore size for nanocomposite reverse osmosis membranes[J]. ACS Appl. Mater. Interfaces, 2020, 12(13): 15765-15773.

[28] Carrasco S, Sanz-Marco A, Matute B M. Fast and robust synthesis of metalated PCN-222 and their catalytic performance in cycloaddition reactions with CO_2[J]. Organometallics, 2019, 38(18): 3429-3435.

[29] Tan W L, Wei T, Huo J, Loubidi M, Liu T T, Liang Y, Deng L B. Electrostatic interaction-induced formation of enzyme-on-MOF as chemo-biocatalyst for cascade reaction with unexpectedly acidstable catalytic performance [J]. ACS Appl. Mater. Interfaces, 2019, 11(40): 36782-36788.

[30] Chen S, Tian J N, Jiang Y X, Zhao Y C, Zhang J N, Zhao S L. A one-step selective fluorescence turn-on detection of cysteine and homocysteine based on a facile CdTe/CdS quantum dots-phenanthroline system[J]. Anal. Chim. Acta, 2013, 787: 181-188.

[31] Beitollahi H, Zaimbashi R, Mahani M T, Tajik S. A label-free aptasensor for highly sensitive detection of homocysteine based on gold nanoparticles[J]. Bioelectrochemistry, 2020, 134: 107497.

[32] Tang L J, Shi J Z, Huang Z L, Yan X M, Zhang Q, Zhong K L, Hou S H, Bian Y J. An ESIPT-based fluorescent probe for selective detection of homocysteine and its application in live-cell imaging[J]. Tetrahedron Lett., 2016, 57(47): 5227-5231.

Photoelectrochemical Sensing Based on Zr-MOFs for Homocysteine Detection

Wen-Xia Dong[1,2], Guang-Ming Wen[1,2*], Bin Liu[2], Zhong-Ping Li[2]

(*1. School of Chemistry and Chemical Engineering, Jinzhong University, Jinzhong, 030600, Shanxi, China; 2. Institute of Environmental Science and School of Chemistry and Chemical Engineering, Shanxi University, Taiyuan 030006, Shanxi, China*)

Abstract: Due to the independent form of the light source and detection system, photoelectrochemical (PEC) sensor has the advantages of low background, high sensitivity and simple operation. So far, PEC systems have been widely used in the fields including the actual detection of metal ions, biological antibodies or antigens in environmental pollutants. When the photosensitive material is irradiated by a light source with an energy being equal to or greater than its band gap, electrons (e^-) transition occurs from the valence band to the conduction band, leaving a hole (h^+), at the same time, the generated electron-hole pair (e^-/h^+) separate, and migrate to the electrode surface and electrolyte to generate photocurrent or photovoltage. When the target analyte is added, it will interact with its recognition molecule, and affect the separation or migration process of the charge, thereby, causing a change in the photocurrent. Metal organic framework (MOF) is a material composed of metal ions and organic linking groups. They have adjustable porosity, functional surface and massive conjugate back bone. These unique characteristics of MOF have been extensively explored in various fields. Zr-MOFs were synthesized use 4-carboxyphenylporphyrin (TCPP) as the ligand, and metal zirconium (Zr) as the coordination metal. Using Zr-MOFs as the photoelectrically active material, a cathode photoelectrochemical sensor was constructed to detect homocysteine (Hcy). A three-electrode system, consisting of Zr-MOFs/FTO electrode, Pt electrode and Ag/AgCl electrode, was inserted into 0.01 mol·L^{-1} HEPES solution to prepare the sensor. An aqueous solution of homocysteine was added to the electrolyte, allowing it to stand for 5 min. Cyclic voltammetry and electrochemical impedance spectroscopy were used to characterize the reaction process and the electron transfer process between optoelectronic materials. When the Xe lamp with $\lambda >$ 420 nm is used to irradiate Zr-MOFs, electrons (e^-) in the valence band transfer to the conduction band, and holes (h^+) are generated in the valence band, thereby, generating light current. The addition of homocysteine will hinder the transfer of electrons, causing the cathode photocurrent to be decreased. The prepared sensor had good linear responses in the ranges of 10 ~ 100 nmol·L^{-1} and 100 ~ 1000 nmol·L^{-1}, and the detection limit was 2.17 nmol·L^{-1}. The sensor also exhibited good stability and selectivity. The prepared cathode photoelectric sensor could sensitively and efficiently detect homocysteine in milk. The studied high-performance photoelectric active materials and chemical sensing platforms may be important for the design of other chemical sensing platforms and the development of PEC applications.

Key words: cathodic photocurrent; Zr-MOFs; homocysteine